Sensorless FOC vector control for High Performance SPIM Drives using new Super-Twisting BS_PCH and VM SC MRAS observer

NGOC THUY PHAM
Faculty of Electrical Engineering Technology
Industrial University of Ho Chi Minh City (IUH)
Ho Chi Minh City, Vietnam
VIETNAM

Abstract: - In this paper, an improved Backstepping _Port Controlled Hamiltonian (STABS_PCH) nonlinear control structure combined with a Stator Current Based Model Reference Adaptive System speed observer using neural network (VMNN_SC_MRAS) is presented. The STABS_PCH control improves and enhances the performance and robustness of SPIM drives. The combination of STABS_PCH controller with the VMNN_SC_MRAS speed estimator can compensate for the uncertainties of the machine parameters and load disturbances to improve the dynamic performance and of robustness the SPIM sensorless drive systems. The effectiveness of proposal control scheme is validated through Matlab-Simulink.

1 Introduction

Recently, the multiphase motor drives are widely used in much applications due to their inherent features such as higher torque density, fault tolerance, greater efficiency, reduced torque pulsations, especially, in some applications such as locomotive traction, electrical ship propulsion, in high power applications such as automotive, aerospace, military and nuclear [1].

Now, SPIM drive systems have been withly applied in industries. In order to improve the performance of the SPIM drive system, many modern control solutions have been developed, among these mothods, FOC Control is a method with many outstanding advantages and is widely applied in SPIMdrive system. The traditional FOC strategies using PI control cannot provide satisfactory quality for high performance SPIM drives so the recently nonlinear control methods have been developed to replace PID controllers [2]. The nonlinear techniques have been proposed for SPIM drive systems such as feedback linearizing control control, slip model control theory (SM), Backstepping control (BS), Fuzzy Logic (FL) control and neural network control (NN), prediction control, passive control, Hamiltonia control [3-18],. v..v.

Among these techniques, the BS control has received great attention due to its systematic and recursive design methodology for nonlinear feedback control. The BS control design can be used to force a nonlinear system to behave like a linear system in a new set of coordinates. The major advantages are that it has the flexibility to avoid cancelations of useful nonlinearities and pursues the objectives of stabilization and tracking. However, the detailed and accurate informations about system dynamics are required when designing traditional BS controllers. To overcome this drawback many strategies have been proposed, in [18] the authors proposed a new BS control scheme using a dynamical induction motor model based on the tranditional BS control with the unknown of the damping coefficient, the motor inertia, the load torque and the uncertainty of the machine parameters. However, the phenomenon of speed ripple and the performance of the reference speed tracking are not good. In [19,21], an integral version of the control and an adaptive observer using the backstepping technique was proposed. The results show the control law and the observer give good performance but it is the complexity of solving differential equations due to the increased number of states of the model. In [21], BS design scheme was developed a for both the control and observer, by adding the integral error tracking component, this method for good dynamic response, precise controls. However, the torque ripple is recorded as quite large, the performance at low speed range and regenerating modes not reported. In this paper, to overcome above the drawbacks, an adaptive BS control is combined with super-twisting algorithm (STABS) for the

output of the speed and rotor flux loop. The STA_BS controller, beside adding the integral error tracking component to improve its sustainability, it also uses well-known super-twisting algorithm to increase its robustness under the parameter uncertainties and external load disturbances and overcome the chattering problem of the classical sliding-mode techniques. However, in order to enhance more the performance and robustness of FOC technichque, beside the improved BS, the author also combinates STABS method with PCH controller for for inner current control loop to enhance performance and the stability for the drive system. The other side, the implementation of vector FOC requires accurate information about the speed and rotor flux. The recent trend eliminate the mechanical sensors used to measure speed because they are sensitive, cause noise, increase cost, size, weight and reduce reliability [22]. In this paper, the authors has focused on the accurate rotor flux estimation, and estimated the speed by the improved stator current based on reference model adaptive systemt (SC_MRAS) using neuron network to improve the performance of observer and controller for the high performance SPIM drives. In detail, in the proposed NN_SC_MRAS observer, the reference model uses the stator current components to free of pure integration problems and insensitive to motor parameter variations. In this SC_MRAS scheme are, first: Adaptive model uses a two layer linear NN, which is trained online by a linear LS algorithm, this algorithm requires the less computation effort and overcome some drawbacks, which cause by its inherent nonlinearity as in literature published before [23]. These significantly improve the performance of the proposed NN_SC_MRAS observer, in addition, using VM will avoid the instability in the regenerating mode [24]. In this proposed, rotor resistance value also has been estimated based on its variation proportional to that one of stator resistance, then the estimated resistance values were updated for the current observer to estimate the current exactly more, and finaly, the adaptive model uses the modified Euler integration to solve the instability problems due to the discretization of the rotor equations of the machine enhance the performance of observer. The combination of the STABS_PCH controller with the proposed SC_MRAS speed estimator increases stability, compensates for the uncertainty caused by SPIM parameter variations, measurement errors and external load disturbances. The effectiveness of this proposed control and observer structure is verified by simulation using MATLAB/ Simulink. The paper is consist of five sections, Section 2 presents the model of the SPIM

drives. Section 3 introduces SATBS_ SM controller, SC MRAS observer also is introduced in this part. Simulation and discuss are presented in Section 4. Finally, the concluding is provided in Section 5.

2 Model of SPIM drives

The system consists of SPIM fed by a six-phase Voltage Source Inverter (VSI). The SPIM drive is show as in Fig.1. By applying the Vector Space Decomposition (VSD) technique introduced in [18], the original six-dimensional space of the machine is transformed into three two-dimensional orthogonal subspaces in the stationary reference frame (D-Q), (x - y) and (zl -z2). The transformation matrix is obtained:

$$T_6 = \frac{1}{\sqrt{3}} \begin{bmatrix} 1 & \frac{\sqrt{3}}{2} & -\frac{1}{2} & -\frac{\sqrt{3}}{2} & -\frac{1}{2} & 0 \\ 0 & \frac{1}{2} & \frac{\sqrt{3}}{2} & \frac{1}{2} & -\frac{\sqrt{3}}{2} & -1 \\ 1 & -\frac{\sqrt{3}}{2} & -\frac{1}{2} & \frac{\sqrt{3}}{2} & -\frac{1}{2} & 0 \\ 0 & \frac{1}{2} & -\frac{\sqrt{3}}{2} & \frac{1}{2} & \frac{\sqrt{3}}{2} & -1 \\ 1 & 0 & 1 & 0 & 1 & 0 \\ 0 & 1 & 0 & 1 & 0 & 1 \end{bmatrix} \quad (1)$$

The electrical matrix equations of SPIM drives in the stationary reference frame may be written as

$$[V_s] = [R_s][I_s] + P([L_s][I_s] + [L_m][I_r])$$
$$0 = [R_r][I_r] + P([L_r][I_r] + [L_m][I_s]) \quad (2)$$

where: [V], [I], [R], [L] and [Lm] are voltage, current, resistant, self and mutual inductance vectors,
respectively. P is differential operator. r and s related to the resistance of rotor and stator respectively. Since the rotor is squirrel cage, [Vr] is equal to zero. The electromechanical conversion only takes in the DQ subspace, (x - y) and (zl -z2) subspace just produce losses. Therefore, the control is based on determining the applied voltage in the DQ reference frame. So SPIM control now is similar to the classical ACIM FOC. The control for the motor in the stationary reference frame is difficult, even for a three phase IM, so the transformation of SPIM model in a dq rotating reference frame to obtain currents with dc components is necessary, a transformation matrix must be used to represent the stationary reference fame (DQ) in the dynamic reference (d-q). This matrix is given:

$$T_{dq} = \begin{bmatrix} \cos(\delta_r) & -\sin(\delta_r) \\ \sin(\delta_r) & \cos(\delta_r) \end{bmatrix} \quad (3)$$

where δr is the rotor angular position referred to the stator that shows in Fig. 1.

The FOC is the most used strategy in the industrial field. In this control method, the rotor flux is controlled by isd stator current component and the torque by isq quadratic component. We have: $\psi_{rq} = 0; \psi_{rd} = \psi_{rd}$. The model motor dynamics is described by the following space vector differential equations:

$$\begin{cases} \dfrac{d\omega}{dt} = \dfrac{3}{2}n_p \dfrac{\delta\sigma L_s}{J}(\psi_{rd}i_{sQ}) - \dfrac{T_L}{J} - B\omega \\[2mm] \dfrac{d\psi_{rd}}{dt} = \dfrac{L_m}{\tau_r}i_{sD} - \dfrac{1}{\tau_r}\psi_{rd} \\[2mm] L_s \dfrac{di_{sD}}{dt} = -ai_{sD} + L_s\omega_s i_{sQ} + bR_r\psi_{rd} + cu_{sD} \\[2mm] L_s \dfrac{di_{sQ}}{dt} = -ai_{sQ} + L_s\omega_s i_{sD} + b_r\omega_r\psi_{rd} + cu_{sQ} \end{cases} \quad (4)$$

where $\sigma = 1 - \dfrac{L_m^2}{L_s L_r}; a = \dfrac{L_m^2 R_r + L_r^2 R_s}{\sigma L_r^2}; c = \dfrac{1}{\sigma}; b = \dfrac{L_m^2 R_r}{\sigma L_r^2}$
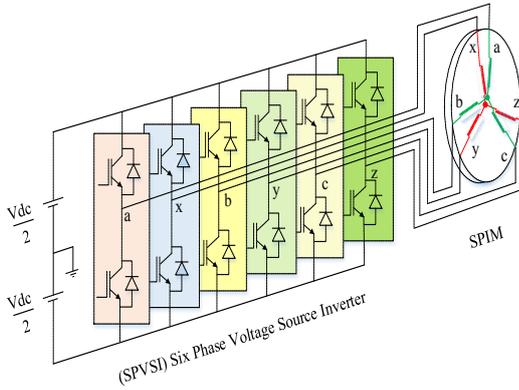

Figure 1. A general scheme of an SPIM drive

The new expression of the electromagnetic torque and the slip frequency are given by:

$$T_e = \frac{3}{2}n_p \frac{M}{L_r}\psi_{rd}i_q \quad (5)$$

$$\omega_{sl} = \frac{M}{L_r}\psi_{rd}i_{sq} \quad (6)$$

3 STABS_PCH control structure for FOC control of SPIM drives:

3.1 STABS design for the outer speed and flux loops:

In this part, an adaptive STA_BS technique is proposed for vector control of SPIM drives. The stability and performance of the control systems is studied using the Lyapunov theory [2]. BS technique is a systematic and recursive method for synthesizing nonlinear control laws. So a virtual command, that will be generated to ensure the convergence of the systems to their equilibrium states. In this proposal, the robustness of this scheme is improved by introducing integral terms of the tracking errors in the control design. Beside this modified BS technique also is combined with super-twisting algorithm (STA_BS) to increase its robustness under the parameter uncertainties and external load disturbances and overcome the chattering problem of the classical sliding-mode techniques.

the rotor flux and speed are the tracking objectives, the tracking errors is defined:

$$\varepsilon_\omega = \omega^* - \omega + k_\omega' \int_0^t (\omega^* - \omega)\,dt$$
$$\varepsilon_\psi = \psi_{rd}^* - \psi_{rd} + k_\psi' \int_0^t (\psi_{rd}^* - \psi_{rd})\,dt \quad (7)$$

The error dynamical equations are

$$\dot{\varepsilon}_\omega = \dot{\omega}^* - \frac{3}{2}n_p \frac{\delta\sigma L_s}{J}\psi_{rd}i_{sq} + \frac{T_l}{J} + B\omega + k_\omega'(\omega^* - \omega)$$
$$\dot{\varepsilon}_\psi = \dot{\psi}_{rd}^* - \frac{L_m}{\tau_r}i_{sd} + \frac{1}{\tau_r}\psi_{rd} + k_\psi'(\psi_{rd}^* - \psi_{rd}) \quad (8)$$

To obtain the virtual controller of speed and rotor flux loop, the following Lyapunov function candidate is considered:

$$V_{(\omega,\psi)} = \frac{1}{2}(\varepsilon_\omega^2 + \varepsilon_\psi^2) \quad (9)$$

Differentiating V:

$$\dot{V}_{(\omega,\psi)} = \varepsilon_\omega \dot{\varepsilon}_\omega + \varepsilon_\psi \dot{\varepsilon}_\psi = \varepsilon_\omega[\dot{\omega}^* - k_t\psi_{rd}i_{sq} + \frac{T_l}{J} + B\omega + k_\omega'(\omega^* - \omega)]$$

$$+ \varepsilon_{\psi_{rd}}\left\{\dot{\psi}_{rd}^* - \frac{L_m}{\tau_r}i_{sd} + \frac{1}{\tau_r}\psi_{rd} + k_\psi'(\psi_{rd}^* - \psi_{rd})\right\} \quad (10)$$

where $k_t = \frac{3}{2}n_p \frac{\delta\sigma L_s}{J}$; k$_\omega$, k$_\Psi$ are positive design constants that determine the closed-loop dynamics. To V' <0, the stabilizing virtual controls are chosen as

$$i_{sq}^* = \frac{1}{k_t\psi_{rd}}\left[k_\omega\varepsilon_\omega + \frac{d\omega_r^*}{dt} + \frac{T_l}{J} + B\omega_r + k_\omega'(\omega_r^* - \omega_r) + \Pi_{\varepsilon_\omega}\right]$$

$$i_{sd}^* = \frac{\tau_r}{L_m}\left[k_\psi\varepsilon_\psi + \frac{d\psi_{rd}^*}{dt} + \frac{1}{\tau_r}\psi_{rd} + k_\psi'(\psi_{rd}^* - \psi_{rd}) + \Pi_{\varepsilon_\psi}\right] \quad (11)$$

where, $\Pi_{\varepsilon_\omega}; \Pi_{\varepsilon_\psi}$ are the control signals injected in order to improved the performance of BS controller. The load torque T$_1$ is estimated:

$$T_L = \frac{1}{1 + \tau_0 p}\left[\left(\frac{3}{2}P\frac{L_m}{L_r}\hat{\psi}_{rd}i_{sq}\right) - \frac{J}{P}\frac{d\omega}{dt}\right]; \quad (13)$$

where: τ_0: is time gain; p: differential.

With Super-Twisting algorithm is used, control law is established as follows:

$$u = -\lambda |S|^{\rho} sat(S) + u_1$$

with: $\quad \dfrac{d}{dt} u_1 = \begin{cases} -u & |u| > U_M \\ -\xi sat(S) & |u| \le U_M \end{cases}$ $\qquad$ (14)

where: $\lambda; \xi; U_M$ là are positive design constants and $0 < \rho \le 0.5$

From Eq. (14), these signals are defined as:

$$\begin{cases} \Pi_{\varepsilon_\omega} = -\lambda_\omega |\varepsilon_\omega|^{0.5} sat(\varepsilon_\omega) - \xi_\omega \int sat(\varepsilon_\omega) dt \\ \Pi_{\varepsilon_\psi} = -\lambda_\psi |\varepsilon_\psi|^{0.5} sat(\varepsilon_\psi) - \xi_\psi \int sat(\varepsilon_\psi) dt \end{cases}$$ $\qquad$ (15)

where, $\lambda_\omega; \lambda_\psi; \xi_\omega; \xi_\psi$ are positive constants.

From (11), (12) and (15), we obtain:

$$\frac{dV_{(\omega,\psi)}}{dt} = -k_\omega \varepsilon_\omega^2 - k_\psi \varepsilon_\psi^2 - \varepsilon_\omega \Pi_{\varepsilon_\omega} - \varepsilon_\psi \Pi_{\varepsilon_\psi} < 0 \quad (16)$$

The virtual controls in (12) are chosen to satisfy the control objectives and also provide references for the next step of the PCH design.

3. 2 The inner current loop controllers using PCH

A PCH system with dissipation is a representation of the form:

$$\begin{cases} \dfrac{dx}{dt} = \left[J(x) - R(x) \right] \dfrac{dH}{dx}(x) + g(x)u \\ y = g^T(x) \dfrac{dH}{dx}(x) \end{cases}$$ $\qquad$ (17)

We define the state vector, input vector and output vector are as follows, respectively

$$\begin{cases} x = \begin{bmatrix} x_1 & x_2 \end{bmatrix}^T = \begin{bmatrix} L_s i_{sd} & L_s i_{sq} \end{bmatrix}^T \\ u = \begin{bmatrix} u_1 & u_2 \end{bmatrix}^T with: u_1 = bR_r \psi_{rd} + cu_{sd}; u_2 = -b\omega_r \psi_{rd} + cu_{sq} \\ y = \begin{bmatrix} i_{sd} & i_{sq} \end{bmatrix}^T \end{cases}$$

The interconnection structure is captured in matrix $g(x)$ and the skew symmetric matrix $J_x = -J_x^T$, $R_x = R_x^T > 0$ represents the dissipation, $H(x)$ is the total stored energy function of the system.

The Hamiltonian function of the system is given by

$$H(x) = \frac{1}{2} x^T D^{-1} x = \frac{1}{2}(x_1^2 + x_2^2) = \frac{1}{2}(L_s i_{sd}^2 + L_s i_{sq}^2); where, D = diag \{L_s \quad L_s\}$$

$\qquad$ (18)

Equation of the SPIM be described in a synchronously rotating dq - reference frame (5) can then be rewritten in the PCH form (17) with:

$$\begin{cases} J(x) = \begin{bmatrix} 0 & L_s \omega_s \\ -L_s \omega_s & 0 \end{bmatrix} \\ R(x) = \begin{bmatrix} a & 0 \\ 0 & a \end{bmatrix}; \quad g(x) = \begin{bmatrix} 1 & 0 \\ 0 & 1 \end{bmatrix} \end{cases}$$ $\qquad$ (19)

Suppose we wish to asymptotically stabilize the system around a desired equilibrium xo, a closed-loop energy function Hd (x) is assigned to the system which has a strict minimum at x0 (that is, Hd (x) > Hd (x0) for all x . x0 in a neighborhood of x0 [17]. Given J(x), R(x), H(x) , g(x) and the desired equilibrium xo. Assume we can find a feedback control u = α(x) , Ra(x) ,Ja(x) and a vector function K(x) satisfying:

$$\left[J_d(x) - R_d(x) \right] K(x) = -\left[J_a(x) - R_a(x) \right] \frac{dH}{dx}(x) + g(x)u$$

$\qquad$ (20)

and such that

$$\frac{dK}{dx}(x) = \left[\frac{dK}{dx}(x) \right]^T;$$
$$K(x_0) = -\frac{dH}{dx}(x_0);$$ $\qquad$ (21)
$$\frac{dK}{dx}(x_0) > \frac{d^2 H}{d^2 x}(x_0);$$

The closed-loop system:

$$\frac{dx}{dt} = \left[J_d(x) - R_d(x) \right] \frac{dH_d}{dx}(x)$$ $\qquad$ (22)

will be a PCH system with dissipation.

$$K(x) = \frac{dH_a}{dx}; H_a(x) = H_d(x) - H(x)$$ $\qquad$ (23)

where H_a is the energy added to the system and x_0 will be a stable equilibrium of the closed-loop system. The expected Hamiltonian energy storage function is defined as

$$H_d(x) = H(x) \quad with: \quad x = x - x_0$$ $\qquad$ (24)

where

$$J_d(x) = J(x) + J_a(x) = -J_d^T(x);$$
$$R_d(x) = R(x) + R_a(x) = R_d^T(x) > 0;$$ $\qquad$ (25)

$$J_a(x) = \begin{bmatrix} 0 & J_1 \\ -J_1 & 0 \end{bmatrix}; R_a(x) = \begin{bmatrix} r_1 & 0 \\ 0 & r_2 \end{bmatrix}$$ $\qquad$ (26)

where, J1 , r1 and r2 are undetermined interconnect and damping parameters. According to equations (20)-(26), the controller of the current inner loop of the motor is

$$\begin{cases} u_{sd} = \sigma \left[ai_{sd}^* + r_1(i_{sd}^* - i_{sd}) - J_1(i_{sq}^* - i_{sq}) - L_s \omega_s i_{sq}^* - bR_r \psi_{rd} \right] \\ u_{sq} = \sigma \left[ai_{sq}^* + r_2(i_{sq}^* - i_{sq}) + J_1(i_{sd}^* - i_{sd}) + L_s \omega_s i_{sd}^* + b\omega_r \psi_{rd} \right] \end{cases}$$

$\qquad$ (27)

The rotor flux ψ_{rd} used in the equation (12), (27) cannot be measured. This component is identified by VM and is presented in section 3.3.3.

3.3 VMNN_SC_ MRAS speed observer
3.3.1 Structure of the VMNN_SC_MRAS Speed Observer

The NNSC_MRAS observer consists of a reference model, an adaptive model, and an adaptation mechanism for estimating speed, which has the

structure diagram as Fig. 5. In the proposed observer, SPIM itself acts as a reference model. The reference components of the VMNN SC_MRAS observer are the measured stator current components. The adaptive model can be calculated from the combined voltage and current models (VM and CM) [17] and is described by the following equation:

$$\dot{x} = Ax + Bu$$
where $\qquad\qquad$ (28)

$$x = \begin{bmatrix} i_{sD} \\ i_{sQ} \end{bmatrix}; A_x = \begin{bmatrix} -\left(R_s + \dfrac{L_m^2}{L_r^2 T_r}\right)\dfrac{1}{\sigma L_s} \\ -\left(R_s + \dfrac{L_m^2}{L_r^2 T_r}\right)\dfrac{1}{\sigma L_s} \end{bmatrix}; B_x = \begin{bmatrix} \dfrac{1}{\sigma L_s} & 0 & \dfrac{1}{\sigma L_s}\dfrac{L_m}{L_r T_r} & \dfrac{1}{\sigma L_s}\dfrac{\omega_r L_m}{L_r} \\ 0 & \dfrac{1}{\sigma L_s} & -\dfrac{1}{\sigma L_s}\dfrac{\omega_r L_m}{L_r} & \dfrac{1}{\sigma L_s}\dfrac{L_m}{L_r T_r} \end{bmatrix}; u_s = \begin{bmatrix} u_{sD} \\ u_{sQ} \\ \psi_{rD} \\ \psi_{rQ} \end{bmatrix}$$
(29)

Its corresponding discrete model is, therefore, given by:

$$\hat{X}(k) = e^{A_x T_s} X(k-1) + \left[e^{A_x T_s} - I \right] A_x^{-1} B_x u_s(k-1) \qquad (29)$$

$e^{A_x T_s}$: is generally computed by truncating its power series ex pansion, i.e.,

$$e^{A_x T_s} = I + \frac{A_x T_s}{1!} + \frac{A_x^2 T_s}{2!} + \dots + \frac{A_x^n T_s}{n!} \qquad (30)$$

If n=1, the simple forward Euler method is obtained, which gives the following finite difference equation [24]

$$\hat{i}_{sD}(k) = w_1 \hat{i}_{sD}(k-1) + w_2 u_{sD}(k-1) + w_3 \hat{\psi}_{rd}(k-1) + w_4 \hat{\psi}_{rq}(k-1)$$

$$\hat{i}_{sQ}(k) = w_1 \hat{i}_{sQ}(k-1) + w_2 u_{sQ}(k-1) + w_3 \hat{\psi}_{rq}(k-1) - w_4 \hat{\psi}_{rd}(k-1)$$
(31)

where marks the variables estimated with the adaptive model and is the current time sample. the weights of the neural networks that can reproduce above equations defined as:

$$w_1 = 1 - \frac{T_s R_s}{\sigma L_s} - \frac{T_s L_m^2}{\sigma L_s L_r T_r}; \; w_2 = \frac{T_s}{\sigma L_s}; \; w_3 = \frac{T_s L_m}{\sigma L_s T_r}; w_4 = \frac{T_s L_m \hat{\omega}_r}{\sigma L_s L_r} \qquad (32)$$

where: $\hat{i}_s(k)$ the current variables estimated with the adaptive model and k is the current time sample, Ts is the sampling time for the stator current observer. The NN has 4 inputs and 2 outputs. In the NN, the weights w1, w2 and w3 are kept constant to their values computed offline while only w4 is adopted online. These equations are the same as those obtained in [17].

In this VMNN_SC_MRAS observer proposed, the adaptive model based on the ADALINE has been improved, A linear least-square algorithm, which is more suitable than a nonlinear one, like the BPN, is used to reduce the computation effort and overcome some drawbacks, which cause by its inherent nonlinearity. Furthermore, the employment of the adaptive model in prediction mode leads to a quicker convergence of the algorithm, a higher bandwidth of the speed control loop, a better behavior at zero-speed, lower speed estimation errors both in transient and steady state conditions.

An integration method more efficient than that used in (29) is the so called modified Euler integration, which also takes into consideration the values of the variables in two previous time steps [17]). Also, in this case, a neural network can reproduce these equations, where and are the weights of the neural networks defined as (33).

Rearranging (33), the matrix equation is obtained in prediction mode. This matrix equation can be solved by any least square technique. Matrix equation (33) can be written: Ax ≈ b, This is a classical matrix equation of the type, where A is called a "data matrix," b is called an "observation vector," and ω_r is the scalar unknown. In this application a classical LS algorithm in a recursive form has been employed; This algorithm is described in detail in [17]. Fig. 2 shows the block diagram of the LS_SC_MRAS speed observer. as we know there are three Least-Squares techniques, i.e. the Ordinary Least-Squares (OLS), the Total Least-Squares (TLS) and the Data Least-Squares(DLS) which arise when errors are respectively present only in b or both in A and in b or only in A. This paper use OLS algorithm: We have:

$$A \hat{\omega}_r(k-1) = b \qquad (35)$$

where

$$A = \begin{bmatrix} \dfrac{3T_s L_m}{2\sigma L_r L_s}\hat{\psi}_{rq}(k-1) - \dfrac{T_s L_m}{2\sigma L_r L_s}\hat{\psi}_{rq}(k-2) \\ -\dfrac{3T_s L_m}{2\sigma L_r L_s}\hat{\psi}_{rd}(k-1) + \dfrac{T_s L_m}{2\sigma L_r L_s}\hat{\psi}_{rd}(k-2) \end{bmatrix}$$

$$b = [W][Y]$$

$$[W] = \begin{bmatrix} 1 & -w_1 & -w_3 & -w_5 & w_7 & -w_2 & w_6 \end{bmatrix}^T$$

$$[Y] = \begin{bmatrix} X & U_s \end{bmatrix}$$

$$[X] = \begin{bmatrix} \hat{i}_{s\alpha}(k) & i_{s\alpha}(k-1) & \hat{\psi}_{rd}(k-1) & i_{s\alpha}(k-2) & \hat{\psi}_{rd}(k-2) \\ \hat{i}_{s\beta}(k) & i_{s\beta}(k-1) & \hat{\psi}_{rq}(k-1) & i_{s\beta}(k-2) & \hat{\psi}_{rq}(k-2) \end{bmatrix}$$

$$[U_s] = \begin{bmatrix} u_{s\alpha}(k-1) & u_{s\alpha}(k-2) \\ u_{s\beta}(k-1) & u_{s\beta}(k-2) \end{bmatrix}$$

3.3.2 Rotor Speed Estimation Algorithm:

Ax ~ b is the linear regression problem under hand. All LS problems have been generalized by using a parameterized formulation (generalized LS) of an error function whose minimization yields the corresponding solution. This error is given by:

$$E_{LS} = \frac{(Ax - b)^T (Ax - b)}{1 - \xi + \xi X^T X} \qquad (36)$$

where T represents the transpose and ξ is equal to 0.5 for TLS, 1 for DLS and 0 for OLS.
Using OLS algorithm, this error is given by:

$$E_{OLS} = (Ax-b)^T(Ax-b) \qquad (37)$$

where:

$$(Ax-b) = \varepsilon = \begin{bmatrix} \varepsilon_{isD} \\ \varepsilon_{isQ} \end{bmatrix} = \begin{bmatrix} i_{sD}(k) - \hat{i}_{sD}(k) \\ i_{sQ}(k) - \hat{i}_{sQ}(k) \end{bmatrix} \qquad (38)$$

This error can be minimized with a gradient descent method:

$$\hat{i}_{sD}(k) = w_1 i_{sD}(k-1) + w_2 u_{sD}(k-1) + w_3 \hat{\psi}_{rd}(k-1) + w_4 \hat{\psi}_{rq}(k-1) + w_5 i_{sD}(k-2) - w_6 u_{sD}(k-2) - w_7 \hat{\psi}_{rD}(k-2) - w_8 \hat{\psi}_{rQ}(k-2)$$

$$\hat{i}_{sQ}(k) = w_1 i_{sQ}(k-1) + w_2 u_{sQ}(k-1) + w_3 \hat{\psi}_{rq}(k-1) - w_4 \hat{\psi}_{rd}(k-1) + w_5 i_{sQ}(k-2) - w_6 u_{sQ}(k-2) - w_7 \hat{\psi}_{rQ}(k-2) + w_8 \hat{\psi}_{rD}(k-2)$$

$$(33)$$

$$w_1 = 1 - \frac{3TR_s}{2\sigma L_s} - \frac{3TL_m^2}{2\sigma L_s L_r T_r}; \quad w_2 = \frac{3T}{2\sigma L_s}; \quad w_3 = \frac{3TL_m}{2\sigma L_s L_r T_r}; \quad w_4 = \frac{3TL_m}{2\sigma L_s L_r}\omega_r; \quad w_5 = \frac{3TR_s}{2\sigma L_s} + \frac{TL_m^2}{2\sigma L_s L_r T_r}; \quad w_6 = \frac{T}{2\sigma L_s}; \quad w_7 = \frac{TL_m}{2\sigma L_s L_r T_r}; \quad w_8 = \frac{TL_m}{2\sigma L_s L_r}\omega_r$$

$$(34)$$

3.3.3 Rotor Flux Estimation and Stator Resistance Online Estimation Algorithm

From (30) can been seen that, the adaptive model generates stator current estimation values based on rotor speed information, stator voltages and rotor flux. In this proposal, from equation VM, the rotor flux values were generated as as follows:

$$\frac{d\hat{\psi}_{rd}}{dt} = \frac{L_r}{L_m}(u_{sD} - R_s i_{sD} - \sigma L_s \frac{di_{sD}}{dt});$$

$$\frac{d\hat{\psi}_{rq}}{dt} = \frac{L_r}{L_m}(u_{sQ} - R_s i_{sQ} - \sigma L_s \frac{di_{sQ}}{dt}); \qquad (41)$$

Eq. (41) show that the rotor flux components are identified from measured stator current and voltage. Using VM to identify rotor flux can be overcome the instability problem in the regenerating mode of operation. From (38) is easy see that, the resistance parameters necessary for estimating the speed. However, during motor operation, these parameters will change with the increase of temperature, especially, at low speed. Therefore to the performance improvement of the observer, especially at low speed, the resistances online identification is necessary.
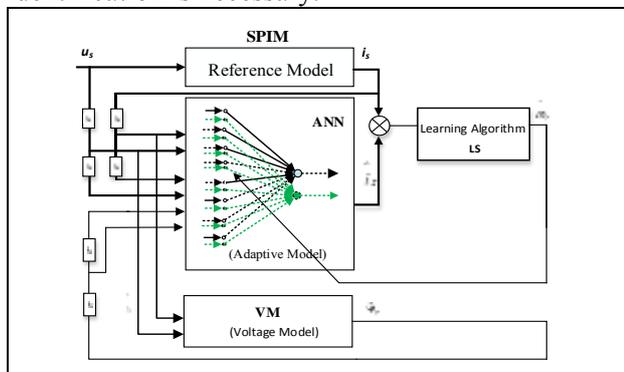
In particular Rs is estimated on the basis of the i_{sD}, i_{sD} measured and $\hat{i}_{sD}, \hat{i}_{sQ}$ estimated stator current components, by means of the following update law:

$$\omega_r(k+1) = \omega_r(k) - \eta\gamma(k)a(k) \qquad (39)$$

where

$$\gamma(k) = a(k)^T a(k) - b(k) \qquad (40)$$

where η is the learning rate, a(k) is the row of A fed at instant k, and b(k) is the corresponding observation.

$$\frac{d\hat{R}_s}{dt} = -\mu((i_{sD} - \hat{i}_{sD})\hat{i}_{sD} + (i_{sQ} - \hat{i}_{sQ})\hat{i}_{sQ}) \qquad (42)$$

where μ is a properly chosen positive constant. Rr has been estimated based on its variation proportional to that one of the Rs on the basis of the following law:

$$\hat{R}_r = K_r \hat{R}_s \qquad (43)$$

where Kr is the ratio of the rated values of the stator and rotor resistances. The estimated resistance values were update for the current observer to estimate the current exactly more.

4 Simulink and discussion

In order to verify and evaluate the performance of the proposed STABS_PCH novel nonlinear control structure combined with VMNN_SC_MRAS speed observer for the sensorless vector control of SPIM drive system as shown in Fig. 3 has been simulated at different speed ranges through Matlab simulation software. Tests in this section are conducted based on recommended benchmark tests [10-11], [15], [17].

SPIM parameters: 220V, 50 Hz, 4 pole, 1450 rpm. Rs = 10.1Ω, Rr = 9.8546Ω, Ls = 0.833457 H, Lr = 0.830811 H, m = 0.783106H, Ji = 0.0088 kg.m2. Rs is nominal value of stator resistance.
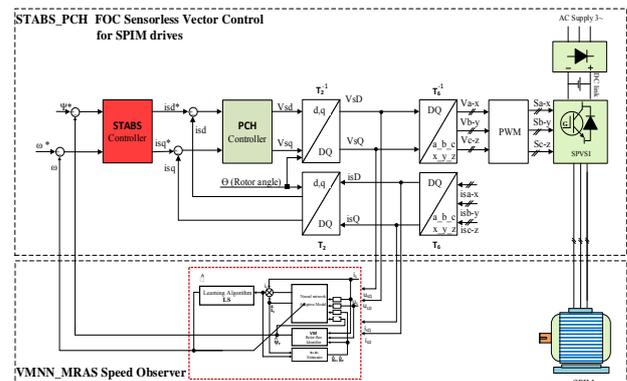
Figure 3. Sensorless vector control of SPIM drive using SATBS_PCH control and VMNN_SC_MRAS observer

In this test, the proposed controller is compared to the feedback linearizing controller [10] and sliding mode controller proposed in [11]. Fig. 4 show the rotor speed, stator current, torque, and rotor flux responses. The reference speed is set up reversal from 100 rad/s to - 100, then speed is surveyed at very low regions (10rad/s) during 2s-3s. The rated load torque is applied at t=1s, and rejected at t = 2.5s and a survey of speed reversal from 150 rad/s to -150 rad/s at 1s, appied in 100% rated load disturbance at 0.5s with the proposed controller and controller in [17] to establish a comparison framework is also also conducted (Figure 5).

The simulaion results show that SPIM give dynamic responses for the proposed controllers have been very well, the overshoot of the speed, torque, stator current and rotor flux in transient modes does not appear. However, observing these responses are easy to see the STABS_PCH controller can provide stability and fast dynamic responses better than the

proposed controllers in [10-11], [15], [17], tracking error and estimate error of almost zero and do not appear the small oscillations as the feedback linearizing controller scheme in [Fig.6,10]; the torque and rotor flux responses also do not appear the overshoot and oscillation as shown in [Fig. 6-7 and Fig. 9, 11]. The transient time and convergence time with reference value of controllers in [10-11], [15], [17] are slower, tracking error increase higher when applying load torque than STABS_PCH controller, in [15] low speed regions surrervey are implemented.

The STABS_PCH proposed control scheme in this paper, the real speed follows the reference speed, the speed tracking efficiency is very high even having the sudden change of load torque, the reference value convergence time is fast, the torque and isq current respond almost instantly. The torque and rotor flux are is also more effectively controlled. The overshoot and oscillation of the torque and rotor flux responses do not been recorded. The torque and isq current respond almost instantly. The rotor flux has been controlled very well and been keep by constant during the survey process.
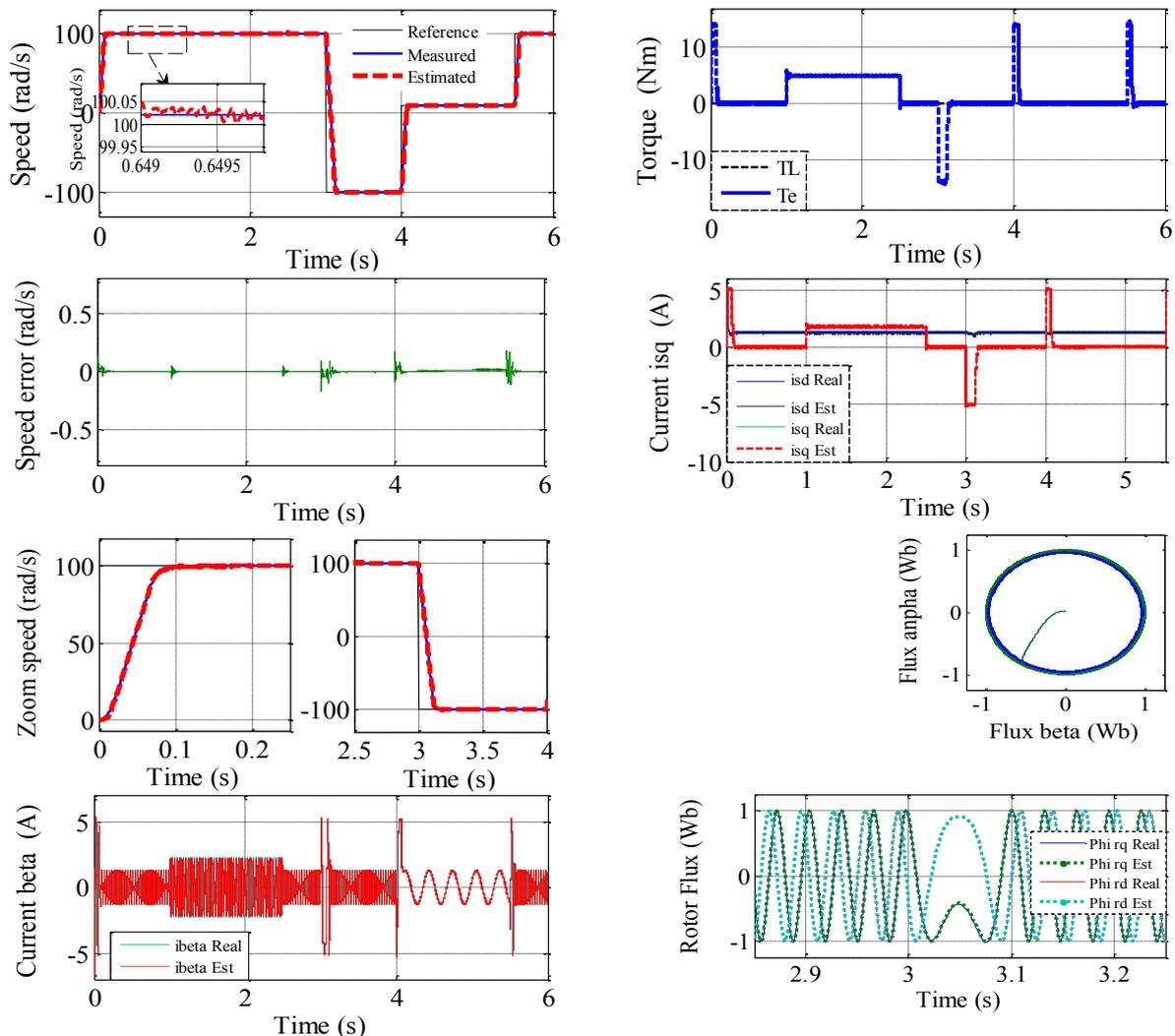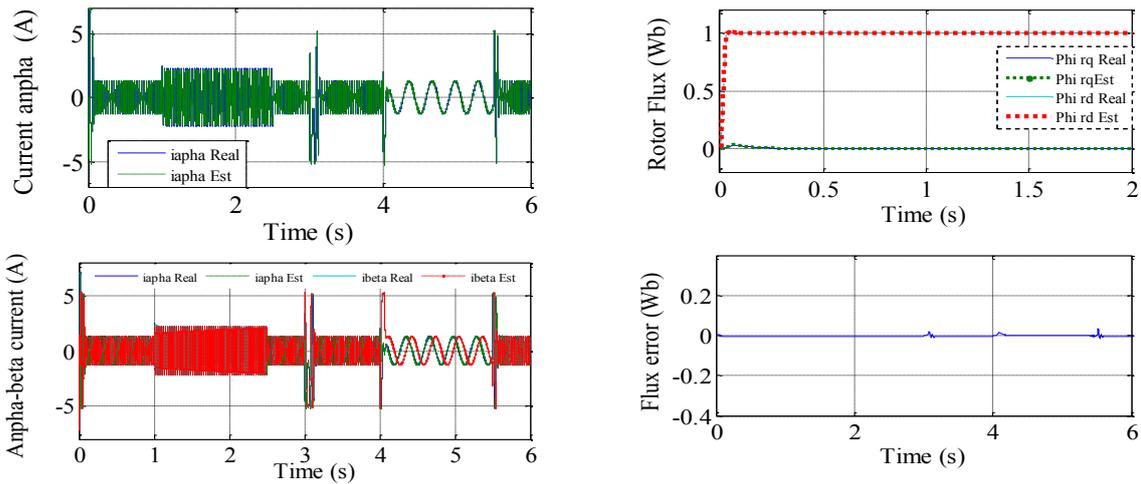
Fig. 4 The speed, torque, stator current, rotor flux responses and estimated error in case of the speed and torque change of STABS_

From the above analys show that the dynamic performance of STABS_PCH controller of the vector control for SPIM drive combinate with the VMNN_MRAS proposed observer work very good and found superior in different operating condition; such as, a step change in command speed and external load disturbances and work low speed region.

Another survey also is implemented according recommended of Benchmark tests in [6] to confirm the performance and robustness of the proposed STABS_PCH control and speed observer when operating at low speed range under the load disturbance and regenerating modes. In that, the reference speed set at the initial time from 0 to 0.5 seconds is zero, after increasing to 10 rad/s and is kept constant at this value and is set to reverse from 10 rad/s to - 10 rad/s at 1.5 s and kept constant until 3.5 s reversed from - 10 rad/s to 2 rad/s and kept at this value until 5.8 s and so on continuously set to reverse from 2 rad/s to - 5 rad/s at 8s, kept constant until 9.25 s, then reduced to 0, and increased again to 5 rad/s at 10s. Specifically: setup time: [0 1.5 3.5 5.8 8 9.25 10 12], reference speed value respectively: [0 10 -10 2 -5 0 5 5].
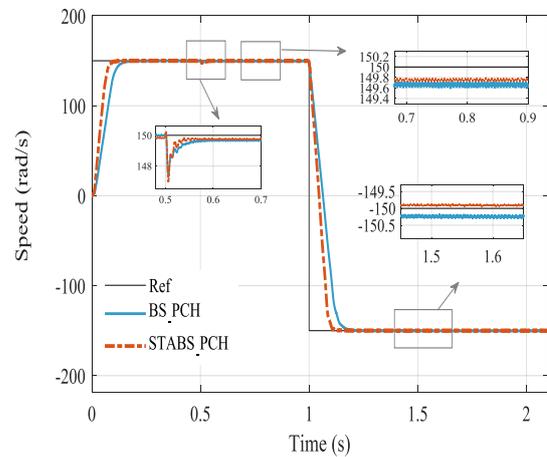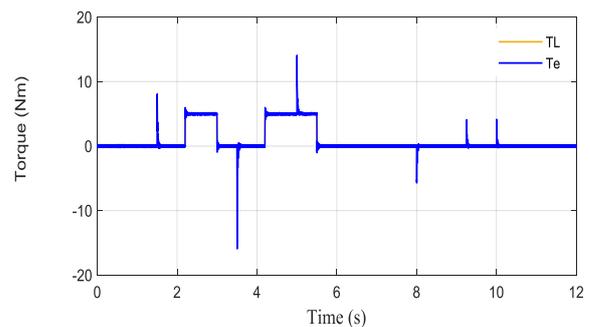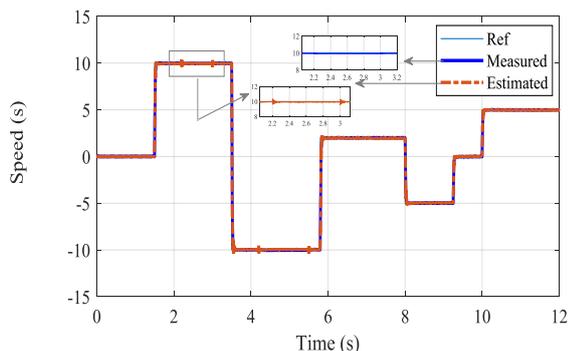

Fig. 5 Compare the speed response of BS_PCH and STA BS_PCH

The simulation results show reference tracking and speed estimation errors are zero even in the zone of unobservability for the interval of [0-1,5s], the speed crosses the zero speed region is very well. SPIM works robust and exactly regenerating modes and load disturbance.
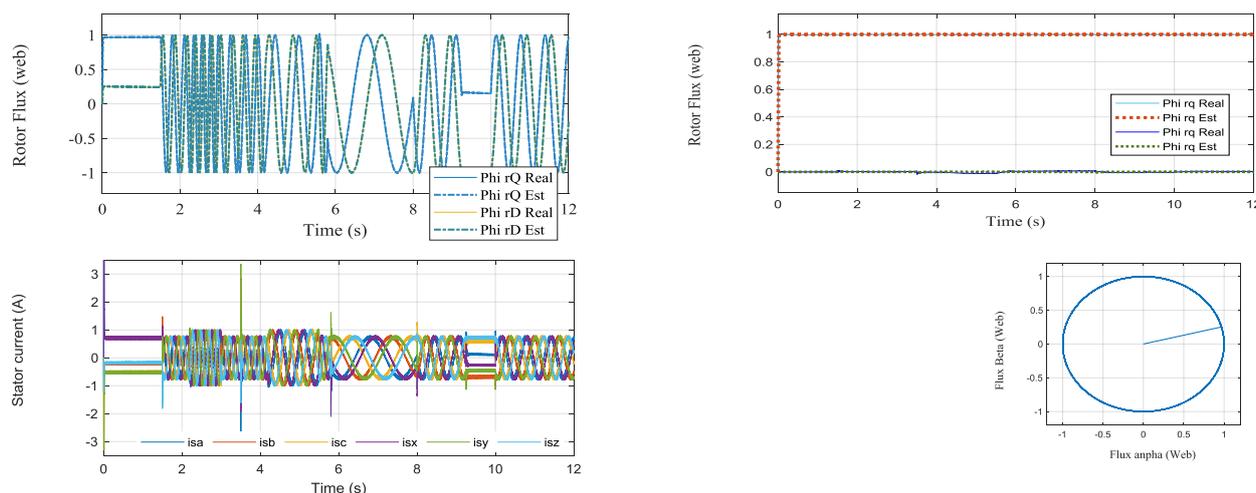
Fig. 5 Speed, Torque, Rotor Flux, Stator current in case of the low speed both motor and regenerating modes

Torque, Rotor Flux, Stator current in case of the low speed both motor and regenerating modes are control very well.

Comparing the survey results of sliding mode controller using FM-MRAS observer controller in [6] show that this proposed controller also give the speed, rotor flux, torque and stator current responses more fast and exactly. The speed, torque and rotor flux responses are fast and follow exactly the reference values. When load disturbances appear in the low speed region, the motor speed is almost unaffected still tracking the reference speed, however, it is easy to see that the STABS_PCH controller get the more accurate speed response, the STABS_PCH controls isq and isd current components are quite well, the torque, current, and flux responses do not appear to scillation phenomenon, observing Fig. 9-10 [6] rippel torque is reported to be quite large.

5 Conclusion

This paper has proposed a novel scheme STABS_PCH nonlinear control for sensorless vector control of SPIM combined with an adaptive VMNN_SCMRAS speed observer. The outer speed and flux loop controllers design is based on the STABS technique using the integral tracking errors action and well-known super-twisting algorithm to increase its robustness under the uncertainties and external load disturbances. PCH controller is used in the inner current loop controller, the stabilization of controller is achieved via system passivity. The closed-loop energy function is equal to the difference between the physical energy of the system and the energy supplied by the controller. On the other hand, in order to guarantee the good performances for the SPIM drives without the use of speed sensor, the FOC vector control combinated VMNN_SCMRAS speed observer. The simulation results show the effectiveness of the proposed control and observer.

References:
[1] E. Levi, Multiphase electric machines for variable-speed applications, *IEEE Transactions on Industrial Electronics*, Vol. 55, No.5, 2008, pp.1893 – 1909.
[2] J. W. Finch and D. Giaouris, "Controlled AC electrical drives," *IEEE Trans. Ind. Electron.*, Vol. 55, No.2, 2008, pp. 481–491.
[3] F. Alonge, M. Cirrincione, M. Pucci and A. Sferlazza, "Input–Output Feedback Linearization Control With On-Line MRAS-Based Inductor Resistance Estimation of Linear Induction Motors Including the Dynamic End Effects," *IEEE Transactions on Industry Applications*, Vol. 55, No.1, 2016, pp. 254-266.
[4]   H. A. Abbasa, M. Belkheirib, B.Zegninia, Feedback Linearization Control of An Induction Machine Augmented by Single Hidden Layer Neural Networks, *International Journal of Control*, DOI: http://dx.doi.org/10.1080/00207179.2015.1063 162, 2015, pp.140-155.
[5] T. Orlowska-Kowalska, M. Dybkowski and K. Szabat, "Adaptive Sliding-Mode Neuro-Fuzzy

Control of the Two-Mass Induction Motor Drive Without Mechanical Sensors," *IEEE Transactions on Industrial Electronics*, 57(2), pp. 553-564, Feb. 2010

[6] M. Touam, M. Chenafa, S. Chekroun, R. Salim, Sensorless nonlinear sliding mode control of the induction machine at very low speed using FM-MRAS observer, *International Journal of Power Electronics and Drive Systems*, Vol.12, No.4. 2021, pp. 1987-1998.

[7] Tohidi, A., Shamsaddinlou, A., Sedigh, A.K.: "Multivariable input-output linearization sliding mode control of DFIG based wind energy conversion system", *9th Asian Control Conf. (ASCC)*, pp. 1–6, June 2013.

[8] Y. Tan, J. Chang, H. Tan, "Adaptive back-stepping control and friction compensation for AC servo with inertia and load uncertainties," *IEEE Transactions on Industrial Electronics*, 50, 2003, pp. 944-952.

[9] M.R Jovanovic, B. Bamieh, "Architecture Induced by Distributed Backstepping Design", *IEEE Transactions on Automatic Control*, Vol. 52, No.1, 2007, pp. 108 – 113.

[10] A. Sabir, S. Ibrir, "Induction motor speed control using reducedorder model", *AUTOMATIKA*, Vol.59, N0.3, , 2018, pp. 275–286.

[11] Abdelkader Ghezouani, Brahim Gasbaoui, and Jamel Ghouili, "Sliding Mode Observer-based MRAS for Sliding Mode DTC of Induction Motor: Electric Vehicle ", *International Journal on Electrical Engineering and Informatics*, Vol. 11, No.3, 2019, pp. 580-595.

[12] Yassine Zahraoui, Mohamed Akherraz, Alfian Ma, A Comparative Study of Nonlinear Control Schemes for Induction Motor Operation Improvement, *International Journal of Robotics and Control Systems*, Vol. 2, No. 1, 2022, pp. 1-17.

[13] Xingang Fu,, and Shuhui Li, A Novel Neural Network Vector Control Technique for Induction Motor Drive, *IEEE Transactions on Energy Conversion*, Vol. 30, No.4, 2015, pp. 1428 – 1437.

[14] Ying Liu, Shanmei Cheng, Bowen Ning, Yesong Li, Performance enhancement using durational model predictive control combined with backstepping control and disturbance observer for electrical drives, *Journal of Vibration and Control*, DOI: 10.1177/1077546318807018, 2018.

[15] Ngoc Thuy Pham, Discrete-time Sensorless Control Using new BS_SM Controller structure and VM_ SC MRAS Adaptive Speed Observer

for The propulsion system of Ship, *WSEAS Transactions on Systems and Control*, Vol 19, 2020, pp.257-267.

[16] C. Cecati, "Position control of the induction motor using a passivitybased Controller," *IEEE Transactions on Industry Applications,* Vol.36, 2000, pp. 1277-1284.

[17] Ngoc Thuy Pham, Khuong Huu Nguyen, "Novel Nonlinear Control Structure for Vector Control of SPIM Drive using BS_PCH ".*International Journal of Power Electronics and Drive Systems* , Vol.11, no.3, 2020.

[18] Hou-Tsan Lee, Fu Li-Chen, Lian Feng-Li. Sensorless adaptive backstepping speed control of induction motor. In: *Proceedings of the 45th IEEE conference on decision and control.* USA;, 13–15 December 2006. pp. 1252–1257.

[19] Mehazzem F, Nemmour AL, Reama A, Benalla H. Nonlinear integral backstepping control for induction motors. *In: Proceedings of 2011 international Aegean conference on electrical machines and power electronics and Electromotion Joint Conference (ACEMP)*, 2015, p. 331–36.

[20] Traoré D, De Leon J, Glumineau A. Sensorless induction motor adaptive observer-backstepping controller: experimental robustness tests on low frequencies benchmark. *IET Control Theory Appl,* Vol. 48, no.10, 2010, pp.1989–2002.

[21] Abderrahmen Zaafouri, Chiheb Ben Regaya , Hechmi Ben Azza, Abdelkader Châari, zDSP-based adaptive backstepping using the tracking errors for high-performance sensorless speed control of induction motor drive, *ISA Transactions*, Vol. 60, 2016, pp. 333-347.

[22] Holtz, "Sensorless control of induction motor drives," Proc. of the IEEE, Vol. 90, no.8, 2002, pp. 1359-1394.

[23] Shady M. G., et al., "Stator current model reference adaptive systems speed estimator for regenerating-mode low-speed operation of sensorless induction motor drives*," IET Electr. Power Appl*., Vol. 7, No.7, 2013, pp. 597–606.

Contribution of Individual Authors to the Creation of a Scientific Article (Ghostwriting Policy)
The authors equally contributed in the present research, at all stages from the formulation of the problem to the final findings and solution.

Sources of Funding for Research Presented in a Scientific Article or Scientific Article Itself
No funding was received for conducting this study.

Conflict of Interest
The authors have no conflicts of interest to declare that are relevant to the content of this article.